Tumor Suppressor p16^{INK4A}: Structural Characterization of Wild-Type and Mutant Proteins by NMR and Circular Dichroism†

Anton Tevelev,‡ In-Ja L. Byeon,*,§ Thomas Selby,‡ Karen Ericson,‡ Hee-Jung Kim,|| Vadim Kraynov,⊥ and Ming-Daw Tsai*,#

Departments of Chemistry and Biochemistry, Biophysics Program, and Campus Chemical Instrument Center, The Ohio State University, Columbus, Ohio 43210

Received January 29, 1996; Revised Manuscript Received May 22, 1996⊗

ABSTRACT: The tumor suppressor p16^{INK4A} with eight *N*-terminal amino acids deleted (p16/Δ1−8) was expressed in *Escherichia coli* without any fusion artifacts and purified. The integrity of p16/Δ1−8 was confirmed by mass spectrometry, and its activity was demonstrated by *in vitro* cdk4 inhibition assay. Various physical methods were used to characterize the molecular and structural properties of p16/Δ1−8. The protein was found to oligomerize *in vitro*, as demonstrated by gel electrophoresis, mass spectrometry, and NMR. Various approaches, including changes of concentration and pH, additions of salts, detergents, and various organic solvents, and construction of a C-terminal deletion mutant and a cysteine mutant were used to try to reduce the extent of oligomerization. Only decreasing the protein concentration was found to reduce oligomerization. The affinity between p16 molecules *in vivo* was demonstrated by the yeast two-hybrid system. The protein was found to be very unstable on the basis of urea- and guanidinium chloride-induced denaturation studies monitored by NMR and CD, respectively. Despite these unfavorable properties, total NMR assignments were accomplished with uniform ^{13}C and ^{15}N isotope labeling. All multidimensional NMR experiments were performed at a very low concentration of 0.2 mM. The secondary structure was then determined from the NMR data. The results of NMR and CD studies indicate that the protein is highly α-helical, and the ankyrin repeat sequences show helix−turn−helix structures. This is the first structural information obtained for the important motif of ankyrin repeats. Overall, p16/Δ1−8 appears to be conformationally flexible. In order to understand the structural basis of the functional changes for some mutants existing in tumor cells, several missense mutants of p16/Δ1−8 were constructed. Four of them were expressed at high levels and purified. The molecular and structural properties of these mutants were analyzed by CD and NMR and compared with the corresponding properties of wild-type p16/Δ1−8. The results suggest that the functional changes in P114L and G101W are likely to be related to global conformational changes. In addition, we have demonstrated that the tendency of aggregation increases significantly by a single D84H mutation.

Of the many tumor suppressors that have been discovered in recent years, p16^{INK4A}, also referred to as multiple tumor suppressor 1 (MTS1)[1] and abbreviated as p16 in this report, is probably one of the shortest in history yet one of the most significant in its relationship to cancer. P16 was discovered independently by two groups in 1993: Serrano et al., (1993) cloned the gene based on ability of the protein to bind to cdk4, and Kamb et al., (1994) discovered the gene by positional cloning via analysis of mutations in pedigrees with familial melanoma. It was found that p16 *in vitro* inhibits cdk4 and cdk6, which, in a complex with a regulatory subunit cyclin D (Meyerson & Harlow, 1994; Bates et al., 1994; Kato et al., 1994), phosphorylate certain regulatory proteins including retinoblastoma gene product, pRb (Matsushime et al., 1992). The pRb in its hypophosphorylated form is a cell division inhibitor, and phosphorylation of pRb allows cell cycle progression from the G1 phase to the S phase (Weinberg, 1995; Müller, 1995; Whyte, 1995; Kouzarides, 1995; Dyson, 1994; Suzuki-Takahashi et al., 1995). Thus, p16 arrests the progression of cell cycle by inhibiting cdk4, as demonstrated *in vivo* (Serrano et al., 1995).

P16 has a calculated molecular weight of 16 569. It is composed mainly of four ankyrin repeats (Lux et al., 1990). Since the discovery of p16, other proteins homologous to it

† This work was supported by NIH Grant CA69472 (to M.-D.T.), and by American Cancer Society Grant IRG16−33 (to I.-J.L.B.). This study made use of a Bruker DMX-600 NMR spectrometer at The Ohio State University funded by NIH Grant RR08299 and NSF Grant BIR-9221639, and a Bruker DMX-750 spectrometer at the National Magnetic Resonance Facility (Madison, WI). T.S. and K.E. were supported by GAANN Fellowship.

‡ Department of Chemistry.
§ Campus Chemical Instrument Center.
|| Biophysics Program.
⊥ Department of Biochemistry.
Departments of Chemistry and Biochemistry, Biophysics Program, and Campus Chemical Instrument Center.

⊗ Abstract published in *Advance ACS Abstracts,* July 1, 1996.

[1] Abbreviations: CD, circular dichroism; cdk4, cyclin-dependent kinase 4; cdk6, cyclin-dependent kinase 6; DMF, dimethyl formamide; DMSO, dimethylsulfoxide; DSS, 2,2-dimethyl-2-silapentane-5-sulfonic acid; MALDI-TOF MS, matrix-assisted laser desorption/ionization time-of-flight mass spectrometry; MES, 4-morpholineethanesulfonic acid; MTS1, multiple tumor suppressor 1; ONPG, *o*-nitrophenyl β-D-galactopyranoside; PMSF, phenylmethanesulfonylfluoride; pRb, retinoblastoma gene product; SDS−PAGE, sodium dodecyl sulfate−polyacrylamide gel electrophoresis; p15^{INK4B} or MTS2, multiple tumor suppressor 2; p16^{INK4A} or p16, inhibitor of cdk4; p16/Δ1−8, p16^{INK4A} with the first eight amino acids deleted; /Δ1−8, /Δ1−51, and /Δ145−156 designate single-deletion mutants, indicating the first and the last amino acids of the deletion; /ΔΔ9−144 and /ΔΔ51−144 designate double-deletion mutants, indicating the first and the last amino acids of the remaining sequence; rt, room temperature; WT, wild type.

S0006-2960(96)00211-5 CCC: $12.00

have been cloned: $p15^{INK4B}$ (MTS2) (Hannon & Beach, 1994), p18 (Guan et al., 1994), p19 (Chan et al., 1995), and their murine analogs (Hirai et al., 1995), including that of p16 itself (Quelle et al., 1995). $P15^{INK4B}$ is the most homologous to p16, with a sequence identity of 80%; it is thought to have the same function as p16 but to be regulated in a different manner (Hannon & Beach, 1994). Functions of p18 and p19 are not known yet. All of these proteins are also homologous to Notch proteins (Greenwald & Rubin, 1992). Of these proteins none has been characterized structurally.

In spite of original doubts (Ohta et al., 1994; Cairns et al., 1994; Wainwright, 1994; Hopkin, 1994), it has now been proven that p16 mutations are involved in the development of different kinds of tumors, including melanoma, esophageal cancer, lung adenocarcinoma, and many others, possibly being their primary cause (Cordon-Cardo, 1995; Hartwell & Kastan, 1994). More than 60 mutant alleles of p16 have been identified in cancer patients [for review, see Cordon-Cardo (1995)], and some have been shown to be functionally impaired *in vitro* and *in vivo* (Koh et al., 1995; Yang et al., 1995; Ranade et al., 1995). Most importantly, it has been demonstrated recently that the phenotype of mice carrying a targeted deletion of the *INK4A* locus develop spontaneous tumors at an early age and are highly sensitive to carcinogenic treatments (Serrano et al., 1996). Hence, p16 is believed to be a good candidate for anticancer gene therapy. Indeed, it causes cell cycle arrest and inhibits tumor cell proliferation in cell culture when transferred into the cells by an adenovirus vector (Jin et al., 1995). Another strategy for therapy of malignancies caused by mutations in the p16 gene would be to design a low-molecular-weight peptide or nonpeptide mimic of p16.

P16 was originally thought to be eight amino acids shorter because of a truncated cDNA clone obtained (Serrano et al., 1993). The originally published sequence also had an erroneous mutation g104t. The full-length sequence was discovered later (Hannon & Beach, 1994) but still contained an error—E2D. The truncated form, designated as p16/Δ1−8 in this report, has been shown to have the same activity as the native p16 (Ranade et al., 1995). In other studies, both p16 and p16/Δ1−8 were expressed only as fusion proteins with either glutathione-*S*-transferase or a six-histidine tag (Serrano et al., 1993; Ranade et al., 1995), not as a free native protein. No structural characterization of p16 or p16/Δ1−8 has been reported to date.

This paper represents our first report on the structure−function analyses of p16. We cloned, expressed, and purified p16/Δ1−8 and related systems, and characterized the molecular and structural properties of p16/Δ1−8 by NMR, CD, and other techniques. The proteins were found to have low solubility, high aggregation tendency, and low stability. Despite these limitations, we completed total NMR assignments of p16/Δ1−8 and determined the secondary structure. The results indicate that the protein is highly α-helical, the global conformation is very flexible, and the important motif of ankyrin repeats exists as helix−turn−helix structures. A number of mutants that have been identified in tumor cells were then constructed and characterized.

MATERIALS AND METHODS

Cloning of p16 and p16/Δ1−8. p16/Δ1−8 was cloned by RT-PCR from total RNA from HeLa cells with primers: GAA CTG CAG CAT ATG GAG CCT TCG GCT GAC and GAC GGA TCC TCA ATC GGG GAT GTC TGA GG using GeneAmp RT-PCR kit (Perkin Elmer) into *Nde*I and *Bam*HI sites of pET-21b phagemid (Novagen). At position 104 in the nucleotide sequence, we had a substitution of G versus T in the sequence, originally published by David Beach and co-workers (Serrano et al., 1993), resulting in a V35G mutation. However, correctness of our sequence was confirmed later by Scott Kern et al. and by Curtis Harris et al. (Caldas et al., 1994; Okamoto et al., 1994). The construct expressed p16/Δ1−8 and was called pET-MTS1/Δ1−8.

Consequently, it was found that the originally published sequence was N-terminally truncated, with the first eight amino acids missing. We constructed the full-length cDNA according to the revised sequence after multiple errors in the originally published sequence were descried (Okamoto et al., 1994; Hannon & Beach, 1994). In order to do that, we amplified truncated cDNA of p16 by PCR from pET-MTS1/Δ1−8 using CGG AAT TCA CCA TGG AGC CCC CGG CGG GGA GCA GCA TGG AGC CTT CGG CTG and the same downstream primer as above and subcloned the product into *Nco*I and *Bam*HI sites of pET-21d (Novagen), resulting in pET-MTS1, a construct expressing full-length p16.

Expression and Purification of p16 and p16/Δ 1−8. *Escherichia coli* B834(DE3) (Doherty et al., 1995) or BL21-(DE3) carrying pET-MTS1/Δ1−8 phagemid were grown in rich medium (19 g/L tryptone, 12 g/L yeast extract and 10 mM $MgCl_2$) with 120 μg/mL ampicillin until $OD_{600} = 0.5-0.6$ and induced with 1 mM IPTG for 6 h at 37 °C.

After cells were harvested, they were broken by sonication in lysis buffer [100 mM Tris-HCl, 10 mM EDTA, 100 mM NaCl, 5 mM β-mercaptoethanol, and 0.5 mM PMSF, pH 7.5 (rt)], at 2 mL/g of cell paste. The lysate was centrifuged for 20 min at 22 000 rpm at 4 °C, and the pellet containing inclusion bodies of the recombinant protein was washed twice with lysis buffer as above (9 mL of lysis buffer per 1 g of original cell paste). The washed inclusion bodies were stirred in solubilization buffer (26.6 mM MES, 1.33 mM EDTA, 8 M urea, and 10 mM DTT, pH did not need adjustment at that point), 9 mL/g of original cell paste, for 1−2 h at room temperature. Suspension was diluted with one-third volume of water and centrifuged for 40 min at 22 000 rpm at 4 °C after pH had been adjusted to 5.68 at room temperature. The supernatant was loaded on a column of SP Sepharose (Pharmacia Biotech) preequilibrated in SPU buffer [20 mM MES, 1 mM EDTA, 6 M urea, and 5 mM β-mercaptoethanol, pH 5.68 (rt)]. The column was washed briefly with the same buffer (at 4 °C) and then excessively washed with SPU buffer containing 20 mM NaCl. p16/Δ1−8 was eluted with 50 mM NaCl in SPU buffer.

Fractions containing p16/Δ1−8 were pooled, Tris-HCl was added to 10 mM, NaCl was added to 140 mM, and urea was added to 8 M final concentrations. pH was adjusted at room temperature to 8.5. This solution was dialyzed against two changes of dialysis buffer [10 mM Tris-HCl, 140 mM NaCl, and 5 mM β-mercaptoethanol, pH 8.0 (rt)]. The dialysis bag was placed in the first buffer change equilibrated to room temperature; then the buffer with the bag was immediately transferred to 4 °C; all subsequent dialysis took place at 4 °C. The solution was further dialyzed against two changes of Q buffer [10 mM Tris-HCl, 5 mM NaCl-, and 5 mM β-mercaptoethanol, pH 8.0 (rt)] at 4 °C. Protein was concentrated on a small (1−2 mL) column of Q

Sepharose (Pharmacia Biotech), preequilibrated in Q buffer, and eluted with a small volume of Q concentration buffer [10 mM Tris-HCl, 1 M NaCl, 1 mM DTT, 5 μM EDTA, pH 8.0 (rt)].

The sample was loaded on Sephadex G-75 or Sephacryl S-100 column (Pharmacia Biotech) preequilibrated with G buffer [4 mM HEPES, 1 mM DTT, 5 μM EDTA, pH 7.0 (rt)]. Fractions containing p16/Δ1−8 were pooled and concentrated in an Amicon stirring cell concentrator using YM-10 membrane and then in a Centriprep-10 (Amicon). The final sample was lyophilized and could be stored at −20 °C for more than a year.

The identity of p16 and p16/Δ1−8 was confirmed by Western blotting using anti-p16 antibodies (Pharmingen). The identity and purity of p16/Δ1−8 were also determined by *N*-terminal amino acid sequencing (which gave MEPSADWLATA for the first 11 amino acids) and by total amino acid analysis which agreed well with calculated amino acid composition (both were performed at W. M. Keck Foundation Biotechnology Resource Laboratory at Yale University). The integrity of the sample was confirmed by MALDI-TOF MS.

Total amino acid analysis was used also to determine the exact concentration of p16/Δ1−8, and consequently, its extinction coefficients: $\epsilon_{220} = 53 \pm 2$ mM^{-1} cm^{-1} and $\epsilon_{280} = 15.5 \pm 0.6$ mM^{-1} cm^{-1} in 4 mM HEPES, 1 mM DTT, and 5 μM EDTA, pH 7.0.

Expression and purification of p16 was performed essentially as described, except that pET-MTS1 phagemid was used and the pH of SPU buffer was 5.5 (rt).

Expression and Purification of Isotope-Labeled p16/Δ1−8. BL21(DE3) cells carrying pET-MTS1/Δ1−8 phagemid were grown in M9 minimal medium with NH_4Cl substituted with $^{15}NH_4Cl$ or with NH_4Cl substituted with $^{15}NH_4Cl$ and glucose substituted with D-glucose-$^{13}C_6$, and containing 120 μg/mL ampicillin, until $OD_{600} = 0.5-0.6$, when they were induced with 1 mM IPTG at 37 °C. After 2 h, rifampicin was added to 50 μg/mL, and cells were grown for another 3 h, as described by James Baleja et al. (Lee et al., 1995). Purification was as described above.

Expression and purification of [^{15}N]Leu/[^{13}C′]Val-labeled and [^{15}N]Gly/[^{13}C′]Leu-labeled p16/Δ1−8 was performed as described for uniform labeling, except that synthetic rich medium with isotopically enriched amino acids ([^{15}N]Leu and [^{13}C′]Val, or [^{15}N]Gly and [^{13}C′]Leu) was used (Muchmore et al., 1989). Purification was as described above.

Cloning, Expression, and Purification of p15 ^{INK4B}. Since the 3′-terminal portion of p15^{INK4B} coding sequence (codons 52−137) shares 97% homology to the corresponding region of p16, it was possible to synthesize p15^{INK4B} cDNA by PCR using a variation of "megaprimer" technique and p16 cDNA in pET-MTS1 phagemid as a template as follows.

The 5′-terminus of p15^{INK4B} cDNA (codons 1−51) bearing little homology to p16 was synthesized by PCR amplification of the annealing product of two primers: CGA TCG TTC GAC ATG CGT GAA GAA AAC AAA GGC ATG CCG TCC GGT GGC GGC AGC GAC GAA GGT CTG GCC ACC CCG GCG CGT GGT CTG GTT GAA and CAT CAT GAC CTG GAT CGC GCG ACG ACC GAA CG GTT AAC ACC GTT CGG GTC CGC GCC AGC TTC CCA GGA GTG ACG AAC TTT TTC AAC CAG ACC ACG. While preserving the native amino acid sequence, the amplified p15^{INK4B} cDNA sequence was altered to ensure optimal conditions for bacterial expression of the protein. This was achieved by substituting poorly translated codons in the sequence with codons translated with high efficiency in *E. coli* (Shpaer, 1986) in the design of the primers. The resultant "megaprimer" had its 3′-end complimentary to codons 49−53 in p16 cDNA. Truncated p15^{INK4B} gene (p15/Δ130−137) was then amplified using the "megaprimer", 3′-end primer 1 (GAC TGA ATT CCC CTG CGA CAT CGC GAT GGC CCC GCT CCT C), annealing to codons 119−127 in p16 cDNA with a single mismatch, and pET-MTS1 phagemid as a template. The final round of PCR included amplification of the full length p15^{INK4B} cDNA using 5′-end primer (CAG TCG TTC CAT ATG CGT GAA GAA AAC), p15/Δ130−137, and 3′-end primer 2 (GAC TGA ATT CAG TCC CCC GTG GCT GTG CGC AGG TAC CCT GCG ACA TCG CG) to account for residual discrepancies between p15^{INK4B} and p16 coding sequences at the 3′-end and to introduce *Nde*I and *Eco*RI restriction sites for subcloning into the expression vector. Amplified full-length p15^{INK4B} cDNA was subcloned into *Nde*I and *Eco*RI sites of pET17b plasmid (Novagen). The resultant pET-MTS2 was used to transform expression host cells BL21 (DE3) pLysS (Novagen). Expression and purification of p15^{INK4B} was performed using methods identical to those described for p16.

Mutant Construction, Expression, and Purification. Mutants were constructed by Kunkel method (Kunkel, 1985) using RZ-1032 *E. coli* (ATCC) and R408 M13 helper phage (Promega) for production of single-stranded uracil-containing DNA. The following primers were used to create mutations: G35V, GGG CAG CGC CAC CGC CTC CAG; D84N, D84H, and D84Y, GGC AGC GTD GTG CAC GGG TCG; G101W, CCA GCC GCG CCC AGG CCC GGT GCA G; P114L, CAG GTC CAC GAG CAG ACG GCC; C72A, GGC GGG GTC GGC GGC ATT CGG CTC CGC GCC G; A127G and A127S, GCG CAG GTA CCG GCY GAC ATC GCG ATG G. Expression and purification of the mutants were as described above, except that SP Sepharose column was developed by a linear 0−100 mM NaCl gradient rather than by the step gradient.

Yeast Two-Hybrid System. pGA-MTS1 was constructed by subcloning a product of PCR amplification of pET-MTS1 with the same primers as for construction of pET-MTS1 into *Eco*RI and *Bam*HI sites of pGAD424 (Clontech).

An amber mutation was introduced at codon 145 in p16 cDNA in pET-MTS1/Δ1−8 by Kunkel mutagenesis, resulting in pET-MTS1/$\Delta\Delta$9−144[1] (primer CTT CCG CGG CAT GCT AGC GGG CAT GGT T). Mutated cDNA was subsequently amplified by PCR, using the same amplification primers as above, and subcloned into *Eco*RI and *Bam*HI sites of pGAD424 resulting in pGA-MTS1/Δ145−156.

To construct pGA-MTS1/Δ1−51 and pGA-MTS1/$\Delta\Delta$52−144,[1] a fragment containing p16 cDNA, obtained by restriction digestion by *Bsp*HI and *Bam*HI of pET-MTS1/Δ1−8 or of pET-MTS1/$\Delta\Delta$9−144, correspondingly, was subcloned into *Nco*I and *Bam*HI sites of pGA-MTS1, replacing the original p16 cDNA in that vector.

To create pAS-MTS1/Δ1−8, a restriction fragment from pET-MTS1/Δ1−8 digest by *Nde*I and *Bam*HI was subcloned into *Nde*I and *Bam*HI sites of pAS-2 (Clontech).

Human cdk4 cDNA was amplified by PCR from pET-cdk4 (will be described elsewhere) with CTG CCA TGG CTA CCT CTC GAT ATG A and CCT GGA TCC TAC TCC GGA TTA CCT TCA TC primers, and subcloned into *Nco*I and *Bam*HI sites of pAS-2. pLAM5′, a plasmid

expressing N-terminal part of lamine C_{66-230} fused to GAL4 DNA binding domain, was from Clontech.

CG1945 strain of *Saccharomyces cerevisiae* (Clontech) was transfected with pAS-2 derivatives, and Y187 (Clontech) *S. cerevisiae* strain was transfected with pGAD424 derivatives. Corresponding transformants were mated with each other; diploids were used for a liquid β-galactosidase assay with ONPG, as described (Clontech).

All DNA manipulation techniques were carried out essentially as described (Sambrook et al., 1989). XL-1 Blue MRF′ *E. coli* (Stratagene) was used as a general host. All DNA constructs were sequenced to check for the absence of errors. Concentrations of p16/Δ1−8 were measured using the extinction coefficient $\epsilon_{280} = 15.5\ mM^{-1}\ cm^{-1}$ determined in the work. Isoelectric points of proteins were determined by isoelectric focusing on a PhastSystem (Pharmacia).

Mass spectrometry was performed at the Campus Chemical Instrumentation Center (The Ohio State University) on Kratos Kompac MALDI3 Reflecting Time-of-Flight Mass Spectrometer. Samples were prepared in 4 mM HEPES, 1 mM DTT, and 5 μM EDTA, pH 7.0, at various protein concentrations.

CD spectra were recorded in 20 mM sodium borate and 40 μM DTT, pH 7.5, on a JASCO J-500C spectrometer.

NMR Sample Preparation. Samples for NMR typically contained 0.2 mM protein, 4 mM HEPES, 1 mM DTT, and 5 μM EDTA in 90% H_2O/10% D_2O or in 100% D_2O at pH 7.0, unless otherwise specified.

NMR Spectroscopy. All NMR experiments were recorded at 27 °C. All NMR experiments, except 4D $^{13}C/^{13}C$-edited NOESY [on a Bruker DMX-750 at the National Magnetic Resonance (Madison, WI)], were conducted on a Bruker DMX-600 at The Ohio State University. Two sets of 3D HNCACB, CBCA(CO)NH spectra were recorded: one on the DMX-600 and the other one on the DMX-750 spectrometer. Both spectrometers were equipped with a 5 mm triple-resonance probe with three-axes gradients. Pulse field gradients were employed to most of the experiments to eliminate artifacts and to suppress the intense water signal (Bax & Pochapsky, 1992) as well as to select for the coherence-transfer pathway (Kay et al., 1992).

COSY, NOESY (t_{mix} = 0.1 and 0.2 s), and TOCSY (t_{mix} = 30.3 and 40.0 ms) experiments were obtained with unlabeled p16/Δ1−8 samples. The water signal was suppressed by presaturation during relaxation delay for samples in D_2O and by 3-9-19 pulse sequence with gradients (Piotto et al., 1992; Sklenar et al., 1993) for samples in H_2O.

2D $^{15}N-^{1}H$ HSQC (Bodenhausen & Ruben, 1980; Bax et al., 1990a) experiments were conducted using the sensitivity enhanced method (Kay et al., 1992) on uniformly as well as specifically ([^{15}N]Leu/[^{13}C′]Val and [^{15}N]Gly/[^{13}C′]Leu) labeled samples in H_2O.

The 3D ^{15}N-edited TOCSY-HSQC and NOESY-HSQC experiments were recorded on uniformly ^{15}N-labeled samples in H_2O. The 3D TOCSY-HSQC was recorded with 25.3-ms mixing period using the MLEV17 mixing sequence (Bax & Davis, 1985) and the sensitivity enhanced method (Kay et al., 1992). The 3D NOESY-HSQC (Sklenar et al., 1993) was recorded with 100-ms mixing period.

The following triple-resonance experiments were recorded on a uniformly $^{13}C/^{15}N$-labeled sample in H_2O: HNCA (Grzesiek & Bax, 1992a), HNCACB (Wittekind & Mueller, 1993; Muhandiran & Kay, 1994), HN(CO)CA (Bax & Ikura, 1991), and CBCA(CO)NH (Grzesiek & Bax, 1992b).

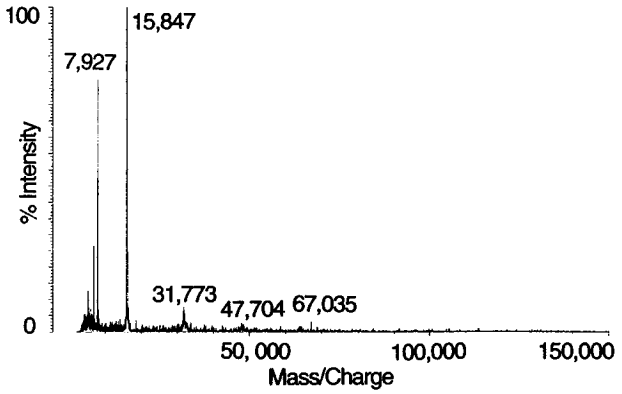

FIGURE 1: MALDI-TOF mass spectrum of p16/Δ1−8. The sample contained 10 μM p16/Δ1−8 in 0.2 mM HEPES (pH 7.0) and 50 μM DTT.

Sensitivity enhanced HCCH-TOCSY (Bax et al., 1990b; Kay et al., 1993) spectra were recorded on a uniformly $^{13}C/^{15}N$-labeled sample in H_2O with 18.7-ms mixing period using the DIPSI-3 mixing sequence (Shaka et al., 1988).

4D $^{13}C/^{15}N$ (Muhandiram et al., 1993) and $^{13}C/^{13}C$ (Vuister et al., 1993) edited NOESY spectra were also recorded on a uniformly $^{13}C/^{15}N$-labeled sample in H_2O with 150-ms mixing period.

Proton and ^{13}C chemical shifts were referenced to internal or external DSS standard at 0.0 ppm since it had been shown to be a better reference for the both nuclei than other possible standards (Wishart et al., 1995). Nitrogen (^{15}N) chemical shifts were referenced to external 1.5 M $(^{15}NH_4)NO_3$ in 1 M HNO_3 at 21.6 ppm (Srinvasan & Lichter, 1977). The acquisition parameters for the NMR experiments are summarized in Table 1 in Supporting Information.

The NMR data were processed on Silicon Graphics Indy and Indigo 2 workstations using XWIN-NMR (ver. 1.1, Bruker) and Felix (ver. 950, Biosym) softwares.

RESULTS

Expression and Purification of p16/Δ1−8. Although p16 and p16/Δ1−8 have been expressed previously in *E. coli* as a glutathione-*S*-transferase or a six-histidine tag-fusion protein (Serrano et al., 1993; Ranade et al., 1995), we decided to express them in their authentic form without any extraneous fusion parts or "tags" to avoid unnecessary complications and distortions in structural analysis. Both the native p16 and the truncated form p16/Δ1−8 were expressed in *E. coli* as described in Materials and Methods. The proteins were expressed in inclusion bodies and were renatured and purified. The identity of both forms was confirmed by Western blotting using anti-p16 antibodies (data not shown). Isoelectric points were determined for the proteins by isoelectric focusing: pI = 5.3 for p16 and 5.5 for p16/Δ1−8.

Since the level of expression of p16 was significantly lower than that of p16/Δ1−8 and since it was reported that the truncated version is as active as the full-length protein (Ranade et al., 1995), we decided to concentrate our work on p16/Δ1−8. The integrity of p16/Δ1−8 was further established by MALDI-TOF MS (Figure 1), which showed a molecular peak of 15.8 kDa, in agreement with the calculated molecular mass of 15.7 kDa within experimental errors. The activity of p16/Δ1−8 was demonstrated by *in vitro* cdk4 inhibition assay, according to the procedure of Hannon and Beach (1994); details will be described elsewhere.

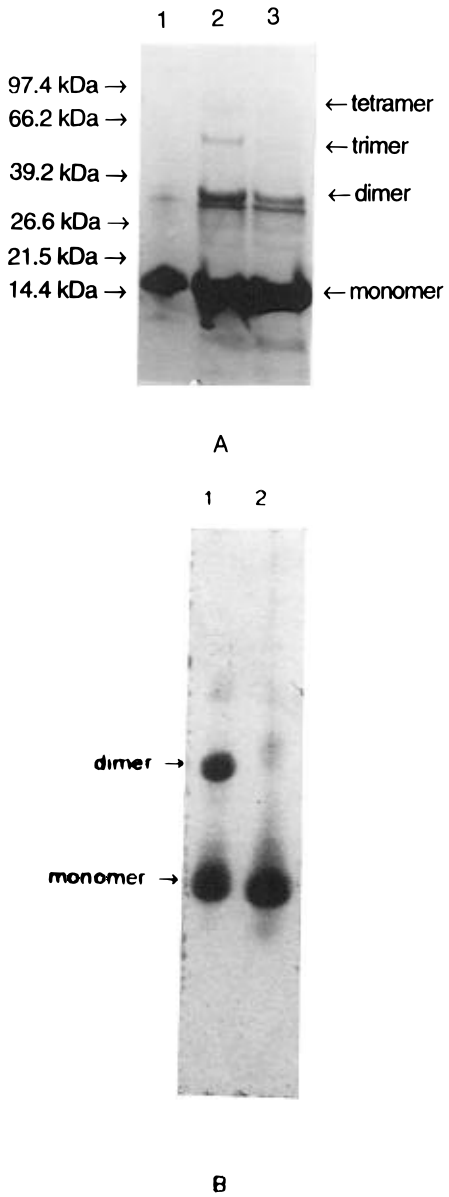

FIGURE 2: Aggregation of p16/Δ1−8 as determined by PAGE. (A) Lane 1, freshly prepared sample of p16/Δ1−8 loaded on the gel without boiling; lane 2, p16/Δ1−8, stored for 5 months in solution at 4 °C, loaded on the gel without boiling; lane 3, the same as lane 2 but boiled in the presence of 100 mM DTT prior to loading on the gel. (B) Lane 1, D84H mutant, stored for 1 day in solution at 4 °C, loaded on the gel without boiling; lane 2, the same as lane 1 but boiled in the presence of 10 mM DTT prior to loading on the gel.

Molecular Properties of p16/Δ1−8. For the purpose of structural and functional studies, it is important to establish whether the protein exists as monomers or oligomers. As shown in Figure 1, the mass spectrum clearly indicates the existence of a dimer with a size of 31.8 kDa, a trimer of 47.7 kDa, and a tetramer of 67.0 kDa. The existence of dimer, trimer, and tetramer was also verified by nondenaturing SDS−PAGE, as shown in Figure 2A, lane 2. Even boiling in the presence of 100 mM DTT did not completely remove oligomerization (lane 3). Neither MALDI-TOF mass spectrum nor SDS−PAGE is a good method for quantitative evaluation of the oligomerization. However, the results taken together suggest that the oligomerization of p16/Δ1−8 is caused either by covalent bonding or by very tight noncovalent interactions.

Table 1: *In Vivo* Oligomerization of p16[a]

Binding of p16 to:	DNA constructs used[b]	% of β-galactosidase activity relative to p16-cdk4[c]	% of β-galactosidase activity relative to p16-p16/Δ1-8[c]
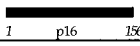 1 p16 156	pGA-MTS1	55 ± 3.8	100 ± 14
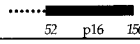 52 p16 156	pGA-MTS1/Δ1-51	44 ± 1.6	80 ± 8
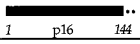 1 p16 144	pGA-MTS1/Δ145-156	50 ± 0.7	91 ± 8
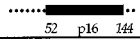 52 p16 144	pGA-MTS1/ΔΔ52-144	44 ± 0.6	80 ± 7
cdk4	pAS-cdk4	100 ± 0.05	

[a] β-Galactosidase activities were measured in CG-1945:Y187 diploids of *S. cerevisiae* using ONPG as a substrate. [b] Specified DNA constructs were used together with pAS-MTS1/Δ1−8, except that, for cdk4, pAS-cdk4 was used with pGA-MTS1. [c] Background β-galactosidase activity measured with pAS-MTS1/Δ1−8 and pLAM5′ was subtracted from presented values.

The tendency of the protein to aggregate was also supported by NMR. Although high resolution 1D NMR spectra of p16/Δ1−8 could be obtained, the sample aggregated with time to give broad resonances. The protein is soluble up to 2 mM, a reasonable concentration for protein NMR; however, at this concentration it aggregates extensively. The maximal concentration at which the protein can give well resolved spectra for 1−2 weeks is 0.2 mM, 10 times lower than the normal concentration for protein NMR. In a separate experiment, the full-length p16 was also shown to aggregate to a similar extent to p16/Δ1−8.

Approaches To Reduce Aggregation by Changing Conditions and Solvents. The protein was always kept in the presence of a reducing agent, DTT (1 mM) or β-mercaptoethanol (5 mM); there was no difference whether DTT was at 1 mM or at a higher concentration. Changing pH or addition of NaCl did not reduce the aggregation. Additions of different organic solvents and detergents—methanol, ethanol, acetonitrile, acetone, DMF, dioxane, DMSO, glycerol, Triton X-100, and octylglucoside—were also tried. None of these reagents was able to prevent aggregation of p16/Δ1−8, as indicated by the line widths of their NMR spectra (not shown).

In Vivo Oligomerization of p16. To verify that aggregation is an inherent property of p16, we measured its oligomerization *in vivo* using the yeast two-hybrid system (Bartel et al., 1993). A copy of p16 fused to the GAL4 DNA binding domain and another copy of p16 fused to the GAL4 activation domain were coexpressed in *S. cerevisiae*. The affinity of one p16 molecule to the other was measured by activation of β-galactosidase reporter gene. The affinity of two p16 molecules was compared with the p16-cdk4 affinity by replacing p16 cDNA in the first construct with cDNA of cdk4. The data shown in Table 1 indicate that there is a high affinity between p16 molecules, sufficient to produce 50% of β-galactosidase activity relative to p16-cdk4 binding. The yeast two-hybrid system sometimes cannot be used with certain systems due to the nature of the particular proteins. However, its applicability to p16 and cdk4 has been previously demonstrated (Serrano et al., 1993). Nevertheless, we used multiple controls to ensure that the observed phenomenon is not an artifact: the β-galactosidase activities in the cells carrying cdk4 alone (pAS-cdk4), p16 alone (pGA-MTS1), p16/Δ1−8 and the N-terminal part of lamine (pAS-MTS1/Δ1−8 and pLAM5′), and p16/ΔΔ52−144 and cdk4

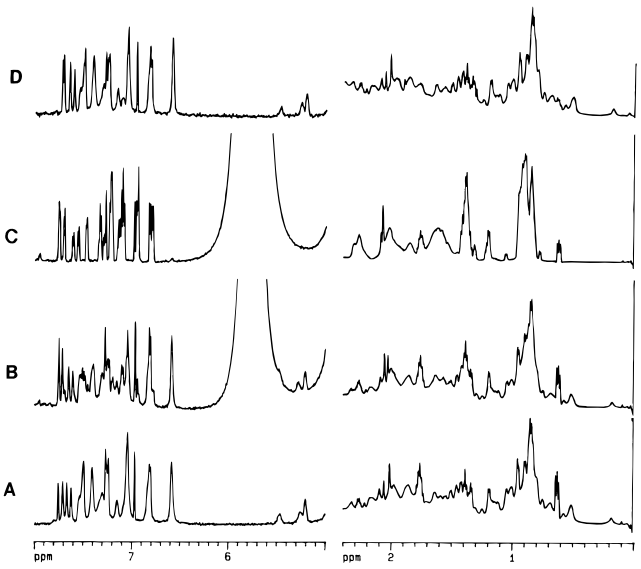

FIGURE 3: 1D ^{1}H NMR spectral titration of p16/Δ1−8 with urea at 600 MHz. (A) Freshly prepared p16/Δ1−8 (0.2 mM) in D_2O without urea. p16/Δ1−8 was titrated with urea: urea concentrations are 1.7 M (B) and 2.9 M (C). Sample C was further titrated with urea (to 3.7 M) and then extensively dialyzed against buffer containing 4 mM HEPES (pH 7.0), 1 mM DTT, and 5 μM EDTA. The dialysate was concentrated to 0.5 mL and lyophilized. The lyophilized protein was dissolved in D_2O and ^{1}H NMR spectrum (D) was recorded. An increased vertical scale (10−12 times) was used for the spectra of the aromatic region (left) compared to those of the aliphatic region (right). The sharp resonance at 0.64 ppm in A−C is arising from an impurity in DSS.

(pGA-MTS1/ΔΔ52−144 and pAS-cdk4) were all at the background level (1 unit/mL). All experiments were repeated at least in triplicate.

To further identify domains responsible for aggregation, we constructed a series of deletion mutants and measured their affinity to full-length p16. As shown in Table 1, deletion of one-third of the entire sequence of p16 (p16/Δ1−51 and p16/ΔΔ52−144 mutants) reduced its self-affinity only to 80%, implying that the main oligomerization site could be located between amino acids 52 and 144.

NMR Analysis of the Stability of p16/Δ1−8. p16/Δ1−8 can be reversibly denatured by addition of urea, as shown on Figure 3. The protein exhibits unchanged NMR spectra up to 1.7 M urea concentration (Figure 3A,B). It changes completely to a random-coil structure at 2.9 M urea concentration (Figure 3C). The result suggests that p16/Δ1−8 is unstable. The growing signal at 5.77 ppm in B and C comes from residual NH protons of urea. Denatured p16/Δ1−8 can be refolded back to the native form by dialysis (Figure 3D).

The reversible denaturation/renaturation provided a way for disaggregation of p16/Δ1−8. Denaturation of an aggregated protein sample by 4 M urea in the presence of 6 mM DTT followed with refolding by dialysis against a buffer containing 4 mM HEPES (pH 7.0), 1 mM DTT, and 5 μM EDTA produced disaggregated p16/Δ1−8, as judged by the ^{1}H NMR spectrum (not shown).

CD Analysis of the Stability and Secondary Structure of p16/Δ1−8. CD was used to quantitatively determine the conformational stability of p16/Δ1−8 by monitoring the denaturation induced by guanidinium chloride. Figure 4A shows the CD spectrum and Figure 4B the denaturation curve of p16/Δ1−8. On the basis of two-state approximation

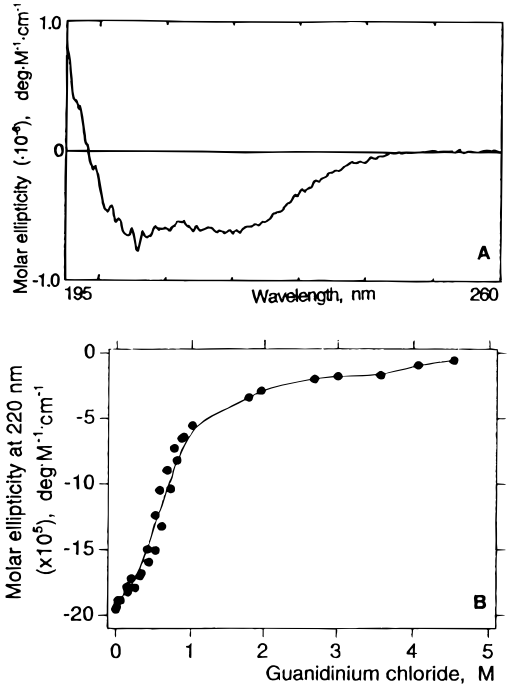

FIGURE 4: (A) CD spectrum of p16/Δ1−8. The sample contained 1.5 μM p16/Δ1−8 in 20 mM sodium borate buffer (pH 7.5) and 40 μM DTT. (B) Denaturation curve of p16/Δ1−8, induced by guanidinium chloride.

Table 2: Conformational Stability of p16/Δ1−8 and Its Mutants[a]

mutant	$D_{1/2}$ (M)	$\Delta G_D^{H_2O}$ (kcal mol^{-1})[b]	m (kcal mol^{-1} M^{-1})[b]
WT	0.7	1.9	2.9
D84N	0.7	1.9	2.6
D84H	0.7	1.6	3.1
P114L	1.3	2.2	1.8
G101W	1.5	2.3	1.8

[a] Samples, containing 7.5 μM protein in 20 mM sodium borate buffer (pH 7.5) and 40 μM DTT, were equilibrated with guanidinium chloride on ice overnight and then shortly equilibrated at 18 °C just prior to CD measurements. Exact guanidinium chloride concentrations were calculated using its refraction index. [b] $\Delta G_D^{H_2O}$ and m values were calculated as described (Pace, 1986).

(Pace, 1986), the denaturation curve gives the concentration of guanidinium chloride at half-denaturation $D_{1/2} = 0.70$ M and the free energy of denaturation in water $\Delta G_D^{H_2O} = 1.9$ kcal/mol (Table 2). The $D_{1/2}$ value agrees with the NMR result (Figure 3) since $D_{1/2}$ for guanidinium chloride is 1.5−2.5 fold lower than the one for urea (Pace, 1986). The value for the majority of proteins falls within 5−15 kcal/mol; thus the result again suggests that p16/Δ1−8 is a relatively unstable protein.

We also undertook CD analysis of the secondary structure of p16/Δ1−8. The CD spectrum in Figure 4A strongly resembles a theoretical curve for an α-helix (Cantor & Schimmel, 1980), which suggests that p16/Δ1−8 has a highly α-helical structure.

General NMR Properties of p16/Δ1−8. The 1D spectrum of p16/Δ1−8 (Figure 3A) shows reasonably narrow ^{1}H lines under the experimental conditions (0.2 mM, pH 7.0). A few $^1H^\alpha$ resonances were observed at a field lower than the water signal, indicating that p16/Δ1−8 may contain some β-strand structures (Wishart et al., 1991). However, the chemical shift dispersion is relatively narrow (0.2−7.8 ppm for a sample in D_2O) and only a few $^1H^N$ protons were subject to slow hydrogen exchange. The ^{15}N−^{1}H HSQC spectrum (Figure

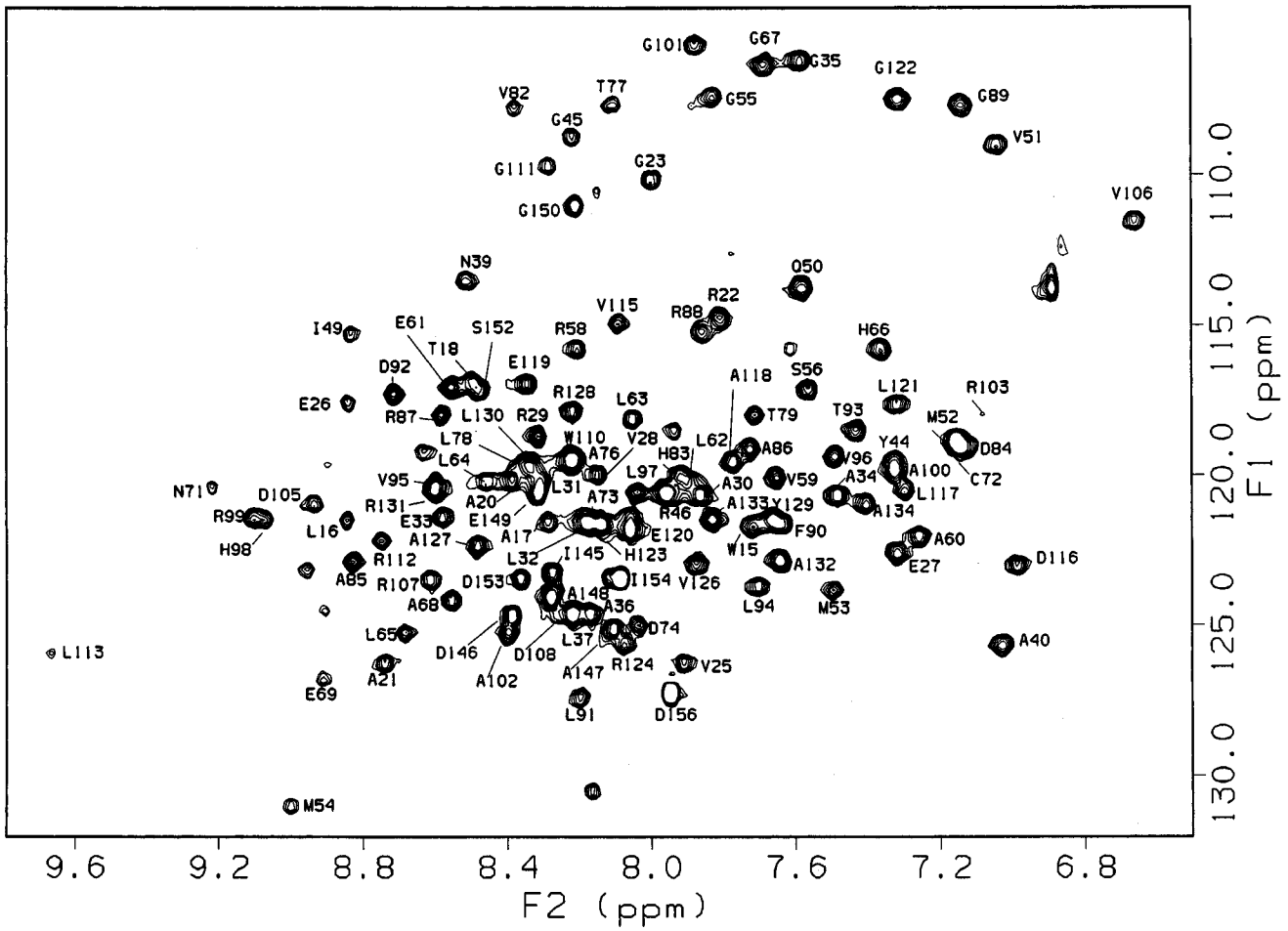

FIGURE 5: $^{15}N-^{1}H$ HSQC spectrum of p16/Δ1−8 at 600 MHz. The assignments are labeled by the one-letter code of amino acids accompanied by a sequence number.

5) also exhibits a relatively narrow dispersion of $^{1}H^{N}$ proton resonance shifts, suggesting that p16/Δ1−8 mainly consists of helical structures. A number of aromatic−aliphatic proton NOE interactions are observed, which contrasts with a low number of detectable aromatic−aromatic interactions (Figure 8A). The only aromatic−aromatic interactions observed in p16/Δ1−8 are between His98 H^{ϵ} and Tyr129 $H^{\delta,\epsilon}$ protons. Interestingly, the indole ring protons of both tryptophan residues (W15 and W110) of p16/Δ1−8 have chemical shifts close to those in a random coiled conformation. No NOEs are observed for the tryptophan residues, which suggests that these residues are likely to be located on the surface of the protein.

Total NMR Assignments of p16/Δ1−8. The spin system identifications of p16/Δ1−8 were obtained as follows: (i) all 17 leucines and 13 glycines were identified from the $^{15}N-^{1}H$ HSQC spectra recorded on selectively [^{15}N]Leu/[^{13}C′]-Val-labeled and [^{15}N]Gly/[^{13}C′]Leu-labeled p16/Δ1−8 samples. (ii) The HNCACB, HNCA, CBCA(CO)NH, and HN(CO)-CA experiments were very informative for identification of spin systems based on their $^{13}C^{\alpha}/^{13}C^{\beta}$ chemical shifts (Grzesiek & Bax, 1992b; Wittekind & Mueller, 1993). (iii) 3D HCCH-TOCSY, as well as homonuclear COSY and TOCSY experiments, were used to identify more spin systems. The 3D ^{15}N-edited TOCSY spectra did not show many long-range correlations, possibly due to large line widths, but showed the $^{15}NH-H^{\alpha}$ correlations for 40% of the protein sequence. Side chain resonances, identified from HCCH-TOCSY, were correlated to the corresponding main chain resonances (^{15}N, $^{1}H^{N}$, $^{13}C^{\alpha}$, $^{1}H^{\alpha}$, $^{13}C^{\beta}$), which had been identified in steps (i) and (ii).

We then proceeded with sequence-specific assignments by identifying sequential $d_{NN}(i,i+1)$ and $d_{\alpha N}(i,i+1)$ NOEs from 3D ^{15}N-edited NOESY-HSQC spectra: 65% of the p16/Δ1−8 residues exhibited sequential $d_{NN}(i,i+1)$ NOEs while only 23% of the protein showed unambiguously recognizable $d_{\alpha N}(i,i+1)$ NOEs. These sequential assignments by NOEs were verified by connecting sequential $^{13}C^{\alpha}/^{13}C^{\beta}$ chemical shifts from the HNCACB, HNCA, CBCA(CO)NH, and HN-(CO)CA experiments. Assignments for the remaining residues were easily obtained solely by the latter experiments based on $^{13}C^{\alpha}/^{13}C^{\beta}$ chemical shifts.

The assigned ^{1}H, ^{13}C, and ^{15}N chemical shifts are listed in Table 2 in the Supporting Information. Approximately 90% of backbone resonances and 70% of side chain resonances have been assigned. Figure 6 summarizes the $d_{NN}(i,i+1)$ connectivities and $d_{\alpha N}(i,i+1)$ connectivities as well as $\Delta^{13}C^{\alpha}$ and $\Delta^{13}C^{\beta}$ which indicate deviations from the random coiled values (Wishart et al., 1995) of the $^{13}C^{\alpha}$ and $^{13}C^{\beta}$ chemical shifts. The information shown in Figure 6 is useful for the determination of the secondary structure as described in the next section.

It is important to note that the primary sequence of p16 consists mainly of four ankyrin repeat units. The importance of this structural motif is addressed in the Discussion. In Figure 6, the amino acid sequences of the ankyrin repeats are represented by regular capital letters, and those outside of the ankyrin repeats are represented by outlined capital

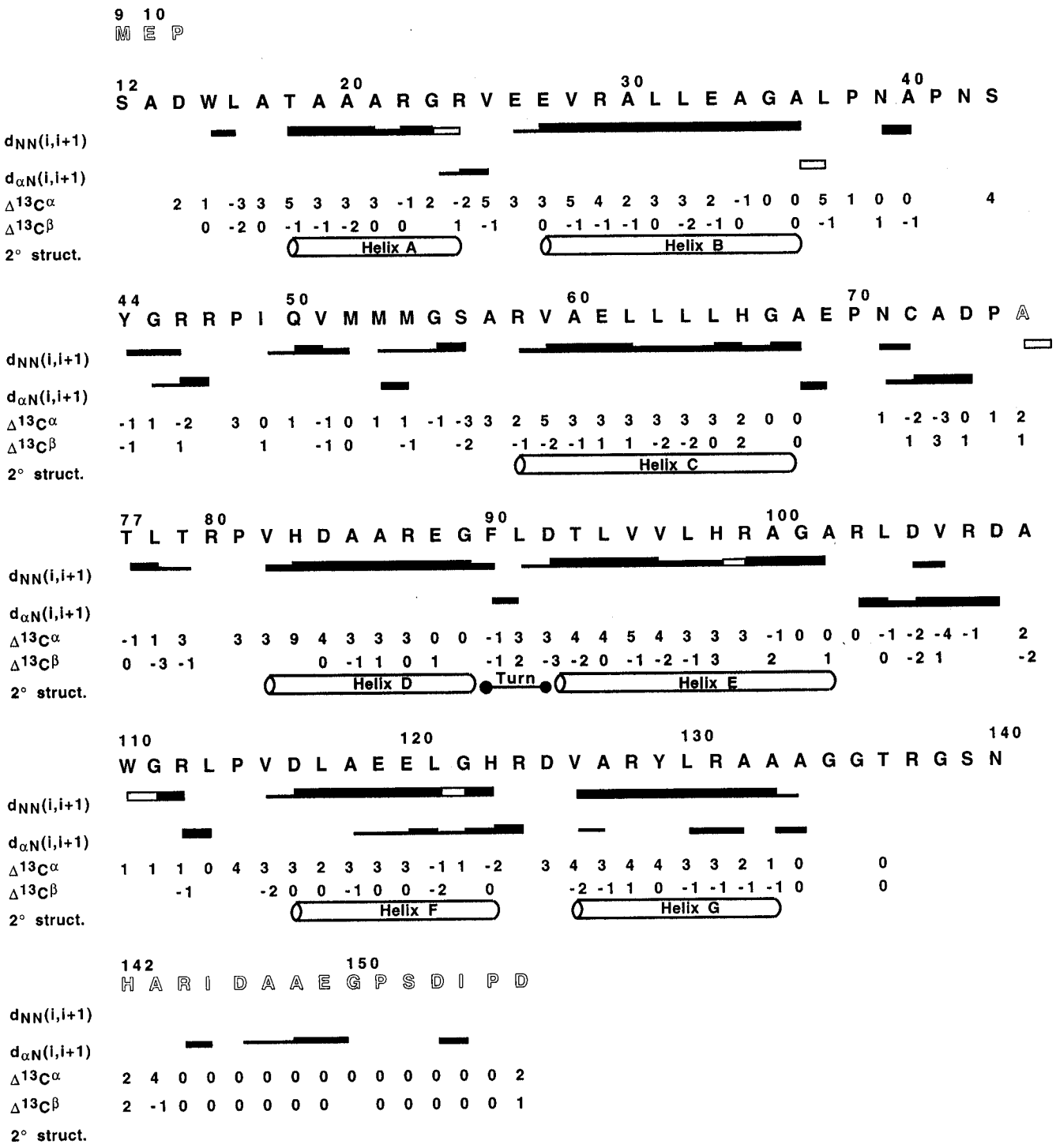

FIGURE 6: Summary of sequential $d_{NN}(i,i+1)$ and $d_{\alpha N}(i,i+1)$ NOEs and $\Delta^{13}C^{\alpha}$ and $\Delta^{13}C^{\beta}$ values of p16/Δ1−8. Also shown are the possible secondary structures derived from these data (see the text). Medium-range NOEs (i to $i+2$, $i+3$, or $i+4$) are not shown here due to the limited number, but they have been described in the text. NOE connectivities that could not be established unambiguously due to spectral overlap are marked by open boxes. The residues of ankyrin repeats are represented in normal letters whereas those outside ankyrin repeats are outlined.

letters. The entire sequence is arranged in a way to allow the four ankyrin repeats to align in parallel.

Secondary Structure Determination of p16/Δ1−8. The NMR assignments allowed determination of the secondary structure of p16/Δ1−8, which is shown in Figure 6 along with the assignment information. The details are explained as follows:

(a) α-Helices. Helical structures are characterized by strong consecutive $d_{NN}(i,i+1)$ NOEs and weak $d_{NN}(i,i+2)$, $d_{\alpha N}(i,i+2)$, $d_{\alpha N}(i,i+3)$, $d_{\alpha\beta}(i,i+3)$, and $d_{\alpha N}(i,i+4)$ NOEs (Wüthrich, 1986). In addition, correlation of $^{13}C^{\alpha}/^{13}C^{\beta}$ chemical shifts to secondary structures has been shown recently: residues which are in a helical structure exhibit downfield-shifted (by 3−4 ppm) $^{13}C^{\alpha}$ signals and upfield-shifted (by 0−1 ppm) $^{13}C^{\beta}$ signals, compared to random-coiled residues (Spera & Bax, 1991). On the contrary, β-strand structures are characterized by strong consecutive $d_{\alpha N}(i,i+1)$ and long-range NOEs, as well as upfield-shifted (by 1−2 ppm) $^{13}C^{\alpha}$ signals and downfield-shifted (by 2−4 ppm) $^{13}C^{\beta}$ signals (Spera & Bax, 1991).

As shown in Figure 6, the following peptide sequences in p16/Δ1−8 are tentatively assigned to have helical structures

due to strong consecutive $d_{NN}(i,i+1)$ NOEs: Thr18−Arg24, Glu27−Ala36, Arg58−Ala68, Val82−Phe90, Asp92−Ala102, Asp116−His123, and Val126−Ala133, all of which are in the middle of the ankyrin repeat units. The majority of these residues indeed exhibit significantly downfield-shifted $^{13}C^{\alpha}$ and slightly upfield-shifted $^{13}C^{\beta}$ signals (Figure 6). However, only a limited though meaningful number of medium-range (i to $i+2$, $i+3$, or $i+4$) NOEs were observed for the helices: (i) $d_{NN}(i,i+2)$ NOEs for Leu32−Ala34, Ala34−Ala36, Ala100−Ala102, and Ala118−Glu120; (ii) $d_{\alpha N}(i,i+3)$ NOEs for Leu32−Glu35, Leu64−Gly67, Asp84−Arg87, Ala86−Gly89, and Val115−Ala118.

(b) Other Secondary Structures. No β-strand structures can be identified for p16/Δ1−8. Cys72−Asp74 and Arg103−Asp108 are the only sequences in p16 which show characteristic NMR properties for β-strand structures: consecutive strong $d_{\alpha N}(i,i+1)$ NOEs, downfield-shifted $^{1}H^{\alpha}$ signals, upfield-shifted $^{13}C^{\alpha}$ signals, and downfield-shifted $^{13}C^{\beta}$ signals. However, no interstrand NOEs can be observed.

The Gly89−Asp92 sequence which is located between helices D and E (Figure 6) can be identified to form a β-turn because of an observable $d_{\alpha N}(i,i+2)$ NOE for Phe90−Asp92. The peptide sequences Arg24−Glu27 and His123−Val126 should also form a turn structure because they are the short linkers for helices A and B and helices F and G, respectively. However, no unambiguous $d_{\alpha N}(i,i+2)$ NOEs can be identified from the sequences.

It is interesting to note that most of the residues at the boundary of the ankyrin repeat units show lack of consecutive $d_{\alpha N}(i,i+1)$ or $d_{NN}(i,i+1)$ NOEs, which suggests that they are in turns or loops. This agrees with the fact that all the prolines in p16 locate at the boundary of the ankyrin repeat units.

(c) C-Terminus. As shown in Figure 6, the C-terminal segment shows little $d_{\alpha N}(i,i+1)$ or $d_{NN}(i,i+1)$ connectivities, and the $^{13}C_{\alpha}$ and $^{13}C_{\beta}$ chemical shifts are little different from the random coil values. The 12 C-terminal residues (Ile145−Asp156) also exhibit intense NH signals in the $^{15}N-^{1}H$ HSQC spectrum shown in Figure 5. These results taken together suggest that the C-terminal residues are likely to exist in a random coil conformation.

Construction of p16/Δ1−8 Mutants. Having characterized the molecular properties and secondary structures of p16/Δ1−8, we proceeded to examine the molecular and structural properties of naturally occurring mutants, aiming at understanding the structural basis of the perturbed functions in these mutants. The following mutants of p16/Δ1−8 were constructed: G35V, D84H, D84N, D84Y, G101W, P114L, A127G, and A127S. All of these mutants have been identified in tumor cells and have been shown to lose some activity on the basis of *in vivo* or *in vitro* assays (see Discussion). Only D84H, D84N, G101W, and P114L were expressed at a level high enough for production of quantities sufficient for structural characterization.

Structural Comparison between WT and Mutants. The four mutants D84N, D84H, P114L, and G101W were first characterized by 1D NMR. As shown in Figure 7, the spectra of D84N (B) and D84H (C) are almost identical to that of WT (A), suggesting a lack of structural perturbation in these two mutants. On the other hand, the spectra of P114L (D) and G101W (E) show severe line broadening and loss of spectral dispersion when compared to that of WT (A). The result of 1D NMR was further confirmed by 2D NOESY spectra shown in Figure 8: the NOESY spectra of

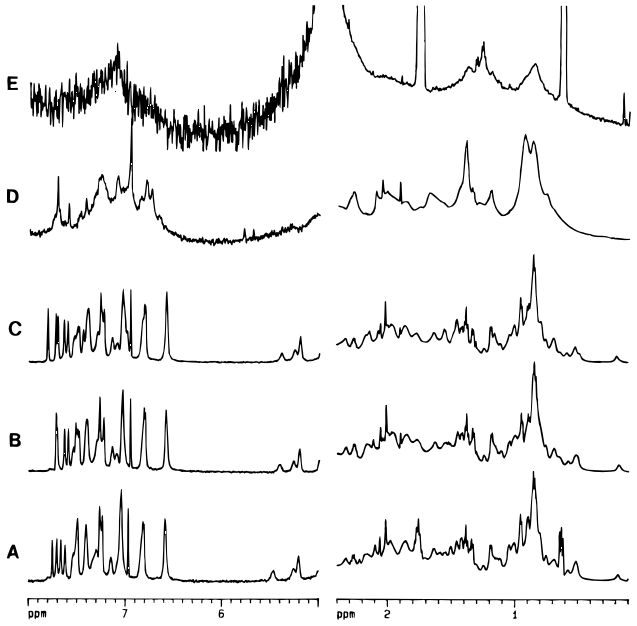

FIGURE 7: Comparison of 1D ^{1}H NMR spectra between p16/Δ1−8 WT and mutants, in D_2O at 600 MHz: (A) WT; (B) D84N; (C) D84H; (D) P114L; (E) G101W. Increased vertical scale (10−12 times) was used for the spectra of the aromatic region (left) compared to those of the aliphatic region (right). The sharp resonance at 0.64 ppm in A is arising from an impurity in the chemical shift standard DSS. The intense lines at 0.60 and 0.72 ppm in E are originated from the excess buffers.

D84N (B) and D84H (C) are almost superimposable to that of WT (A) whereas that of P114L is not. The NOESY spectrum of G101W is not obtained due to a very low solubility. Despite the large changes in the NMR spectra, the less sensitive CD spectra were not perturbed to a noticeable extent in all four mutants, as shown in Figure 9A. The results taken together suggest that the conformations of D84N and D84H are not perturbed relative to that of WT. The structures of P114L and G101W will be addressed in a later section.

Conformational Stability of the Mutants. The conformational stability of the mutants were also determined by guanidinium chloride-induced denaturation and monitored by CD. As shown by the data listed in Table 2, D84H and D84N behave very similarly to WT in the values of $\Delta G_D^{H_2O}$, $D_{1/2}$, and m. These results agree with the NMR results in suggesting that the conformations of these two mutants are unchanged from that of WT. On the other hand, P114L and G101W show significantly lower m values: 1.8 versus 2.9 kcal mol^{-1} M^{-1} for the wild type. It suggests that these two mutants could have significantly altered structures.

Molecular Properties of the Mutants. The broad NMR resonances (even when the samples were freshly prepared) suggest that P114L and G101W aggregate extensively. However, since the global conformation of these two mutants are likely to be perturbed (see Discussion), it is uncertain whether the enhanced aggregation is the result of global structural perturbation or is caused by the site-specific mutation. In the rigorous sense of structure−function analysis, as long as there is evidence of global conformational change in the mutant one cannot directly correlate the changes in other properties to the mutation (Tsai & Yan, 1991).

On the other hand, fresh samples of mutants D84N and D84H display well resolved 1D NMR spectra (Figure 7B,C)

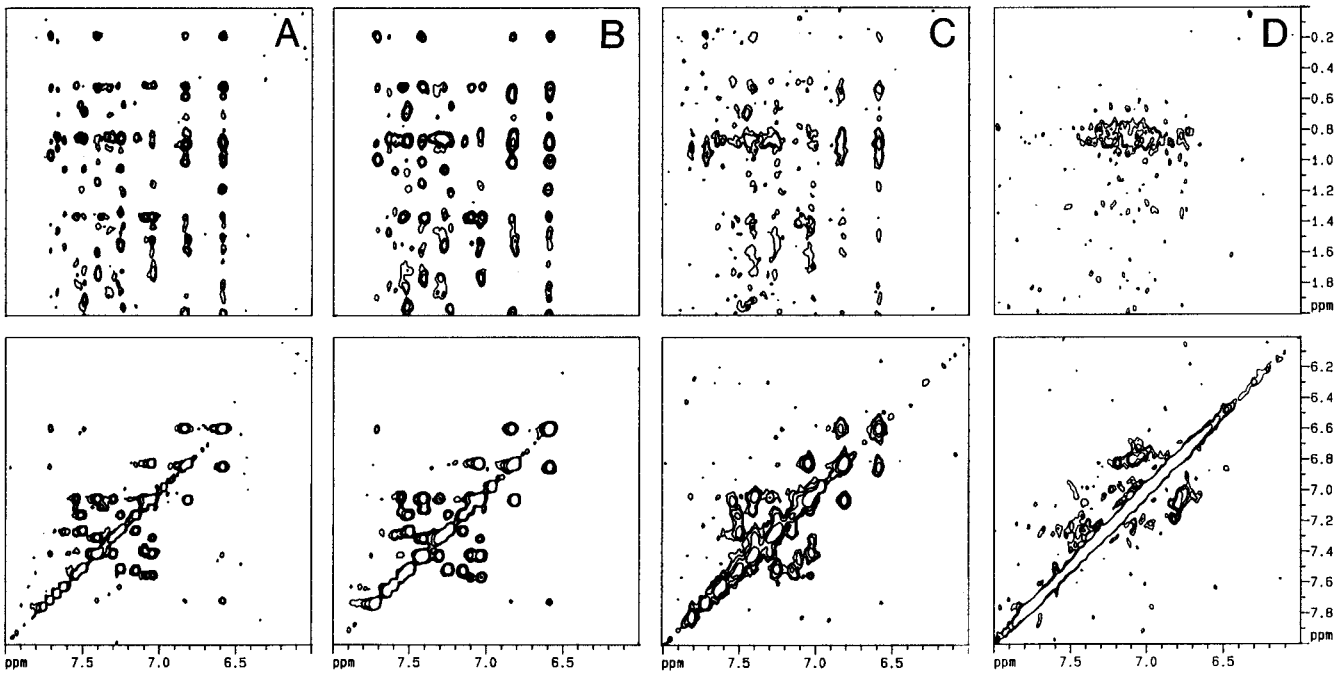

FIGURE 8: Comparison of 2D NOESY spectra between p16/Δ1−8 WT and mutants, in D_2O at 600 MHz: (A) WT; (B) D84N; (C) D84H; (D) P114L. The mixing times for the NOESY spectra are 200 ms for A and B, and 100 ms for C and D.

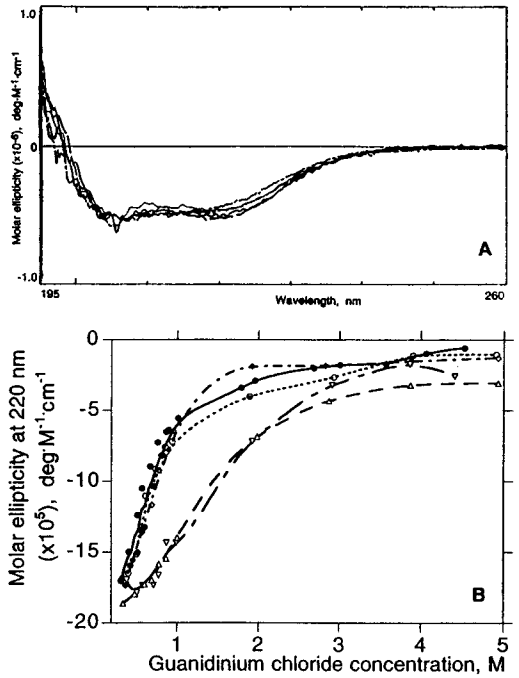

FIGURE 9: (A) Comparison of CD spectra between p16/Δ1−8 WT and mutants: (—) wild type; (− −), D84N; (− - −) D84H; (— - —) P114L; (— - —) G101W. (B) Denaturation curves of mutants: (●) wild type; (◇) D84N; (○) D84H; (△) P114L; (▽) G101W.

nearly identical to the corresponding spectra of WT p16/Δ1−8, suggesting that the conformation of these two mutants are unchanged from that of WT. D84N can keep the well resolved spectral property for 1−2 weeks at a 0.2 mM protein concentration similarly to WT. However, D84H loses the property within a couple of hours and changes to give a spectum with broadened lines but with unperturbed chemical shifts (Figure 10), suggesting that D84H also shows enhanced aggregation. Note that the NMR properties of the aggregated D84H are basically different from those of P114L and G101W. The SDS−PAGE results also show that D84H

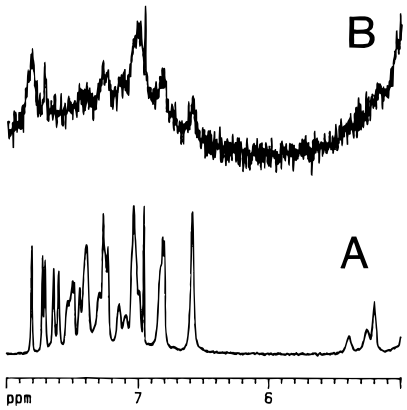

FIGURE 10: Illustration of the tendency toward aggregation of D84H by NMR. Freshly prepared D84H sample was used for the spectrum A; spectrum B was obtained after incubating the sample at room temperature for 2 days.

(Figure 2B) aggregates more extensively than WT (Figure 2A). Since the global conformation of D84H is not perturbed, the enhanced aggregation can be attributed to the site-specific mutation.

Constructions of Mutants to Probe Aggregation. (a) C-Terminus Deletion Mutant. Since the results of NMR studies established that the C-terminus exists as a random coil in solution, we thought that it could be involved in the aggregation of p16/Δ1−8. Therefore, we constructed a mutant with the last 11 C-terminal amino acids of p16/Δ1−8 deleted. The deletion mutant, p16/ΔΔ9−144, exhibited an NMR spectrum (not shown) similar to that of the wild type but aggregated considerably more; it precipitated extensively at 0.1 mM.

(b) p15^{INK4B}. We also cloned, expressed, and purified p15^{INK4B}, which lacks 12 C-terminal residues compared to p16. The 1D NMR spectrum (not shown) suggests that p15^{INK4B} also aggregates extensively. The results in a and b, taken together with the result of the yeast two-hybrid system studies (Table 1), suggest that the C-terminal segment

of p16 may not be responsible for aggregation.

(c) C72A Mutant. Although the aggregation was not limited to dimerization, we still suspected that dimerization caused by disulfide bond formation could lead to further aggregation. To unequivocally test this possibility, we changed the single cysteine residue of p16/Δ1−8 to alanine. The C72A mutant was constructed, purified, and found to give broad NMR signals also (not shown). The results, in conjunction with the fact that aggregation could not be prevented by addition of DTT as described earlier, suggest that disulfide bond formation or thiol oxidation is not the cause of aggregation.

DISCUSSION

The results described in this paper represent the first detailed characterization of the molecular and structural properties of the important tumor suppressor p16. Although most of our work was performed on the truncated form, p16/Δ1−8, due to the low expression level of the full-length protein in *E. coli*, all existing evidence indicates that the structural and functional properties learned from the truncated form should be applicable to the full-length protein. To date, the work from other laboratories has focused on *in vivo* or *in vitro* assays and has used fusion forms of p16 (Serrano et al., 1993; Koh et al., 1995; Yang, 1995). The significance of our structural analyses of p16/Δ1−8 and its mutants is further elaborated in the following sections.

Possible Mechanisms of Aggregation of p16/Δ1−8. Our results indicate that p16/Δ1−8 forms dimers, trimers, and tetramers (and perhaps, undetected higher order oligomers) as a function of time and that the mutants studied aggregate at least as extensively as the WT p16/Δ1−8. The tendency of the full-length p16 to oligomerize *in vivo* was demonstrated using a yeast two-hybrid system. The affinity between p16 molecules was found to be very significant in comparison with the p16-cdk4 affinity. Most of the binding affinity was retained in a deletion mutant consisting of residues 52−144. This result could imply that the primary oligomerization site is located between residues 52 and 144; however, this is a valid interpretation only if the fragment assumes the WT-like structure.

We have ruled out the following two possibilities as the cause of aggregation: interaction between the floppy C-terminal fragments and formation of a disulfide bond between two protein molecules. In our view, there are two possible mechanisms of aggregation: (i) hydrophobic interaction between surface hydrophobic residues, for example, Trp15 and Trp110; and (ii) partial (or local) denaturation followed by aggregation. Since the main function of p16 involves protein−protein interactions (with cdk4), it may be possible that in the absence of cdk4 the protein interacts with another molecule to form a dimer. However, this cannot explain the fact that the aggregation is slow and time-dependent and that oligomers are formed in addition to dimers.

Secondary Structures of p16/Δ1−8. Despite the low stability and the high aggregation tendency of p16/Δ1−8, we have been able to accomplish the total NMR assignment of the protein. All of the multidimensional NMR experiments were performed at only 0.2 mM concentration of the protein, and a typical 3D NMR experiment took 6−8 days. The data are sufficient for the secondary structure determination as shown in Figure 6. However, even the 3D ^{15}N-edited NOESY, which required an acquisition time of 7 days, did not provide enough NOEs to calculate the tertiary structure. The 4D ^{15}N/^{13}C and ^{13}C/^{13}C edited NOESY (7 days each experiment) spectra gave even fewer NOE cross-peaks. The highlights of the structure of p16/Δ1−8 (Figure 6) are described as follows. (i) The four ankyrin repeats in p16/Δ1−8 have very similar secondary structures: each repeat consists of mainly helix−turn−helix structures. Note that the first half of the second ankyrin unit does not show NOE patterns characteristic for helical structures from our current NMR data. However, considering the ankyrin repeat homology and the unfavorable experimental condition (a very low, 0.2 mM, protein concentration), it is possible that the second repeat also has the same structural topology as the others. The significance of the ankyrin repeat structure is elaborated in the following section. (ii) The helix−turn−helix structures are connected by long polypeptides at the boundary of the ankyrin repeats. There is some NOE evidence which indicates that helix B is in contact with C whereas helix E with G. However, it would be premature to draw any conclusion about the global fold of p16/Δ1−8 at the current stage of our NMR studies. (iii) Little β-strand structures are identified in p16/Δ1−8. (iv) The C-terminal residues are likely to exist in a random coil conformation. In agreement with the NMR data, the CD spectrum of p16/Δ1−8 (Figure 4A) shows that the protein has a high content of α-helical structures.

Ankyrin Repeat Structures. The sequence of p16 is almost entirely composed of four ankyrin repeats. Ankyrin repeats are short (about 33 amino acids) stretches present in a variety of vertebrate, invertebrate, yeast, and viral proteins. Among them are human ankyrins which are thought to participate in interactions between cytoskeleton and integral membrane proteins (Lux et al., 1990), bcl-3 human oncogene, p53 binding protein p53BP2 (Helps et al., 1995), *Caenorhabditis elegans* lin-12 (Yochem et al., 1988) and *Drosophila melanogaster* Notch genes (Matsuno et al., 1995), which are involved in regulation of cell differentiation, *Schizosaccharomyces pombe* cdc10 required for cell cycle progression (Aves et al., 1985), *S. cerevisiae* Akr1p protein which is a part of pheromone signaling (Kao et al., 1996), vaccinia 32 kDa protein (Gillard et al., 1986), and many others. Moreover, all proteins of the recently discovered INK4 tumor suppressors family p15^{INK4B}, p18^{INK4C}, and p19^{INK4D} consist of ankyrin repeats. It appears that ankyrin repeats conduct protein−protein interactions but, even until now, nothing is known about structure of this widely represented repetitive motif. Our finding that the core of the ankyrin repeats in p16/Δ1−8 exist in helix−turn−helix structures represents the first structural information of this important structural motif. It should be useful in understanding the structure−function relationship of other proteins containing ankyrin repeats.

Prospects for the Tertiary Structure of p16. Although the total assignments have been nearly completed and the secondary structure has been largely determined, there were not enough medium- and long-range NOE cross-peaks to allow calculation of the tertiary structure of p16/Δ1−8. The paucity of detectable NOEs could be caused by two possible factors: the sensitivity is too low due to the very low concentration (0.2 mM) used in NMR experiments, and/or the protein is conformationally flexible. The low concentration will always lead to less detectable NOE cross-peaks. However, in our view, there is also ample, though indirect, evidence for the second factor: the overall chemical shift

dispersion is relatively narrow, and there are few slowly exchanging amide protons. In addition, an attempt to crystallize the free p16 has not been successful despite an extensive effort by our collaborator (J. Noel, personal communication).

The results taken together suggest that there is a good possibility that p16 is conformational flexible when existing alone in solution. It may not attain a rigid tertiary structure until it binds to its target, cdk4. It is also possible that a certain percentage of dimers exist under the NMR experimental conditions.

Structure−Function Relationship of Mutants. For the mutants which have been demonstrated to have impaired functions structural characterization can provide useful information in three aspects: (i) If the conformation of a mutant is significantly perturbed, structural perturbation should be the cause of the impaired function. (ii) If the conformation of a mutant is not perturbed, the specific mutation should be responsible for the functional change and the mutated residue is likely to be involved in the inhibition of cdk4 (Tsai & Yan, 1991). (iii) Structural characterization of a mutant can enhance understanding of other molecular properties, such as stability and oligomerization. The significance of the results of various mutants is elaborated below.

(a) P114L. This mutant has been shown to be defective in both *in vitro* and *in vivo* experiments (Koh et al., 1995). The NMR spectra in Figures 7−8 suggest that its conformation is significantly perturbed and/or that the protein severely aggregates. Although the two factors could not be dissected quantitatively, there is other evidence that the conformation of this mutant is significantly perturbed: (i) the *m* value in Table 2 is significantly lower relative to WT; (ii) comparison between the spectrum of this mutant and that of the aggregated sample of D84H (Figure 10B) indicates that there are significant differences between the two spectra. Figure 10B clearly retains most of the resonances in the unaggregated form (Figure 10A); on the other hand, the spectrum of P114L (Figure 7D) does not resemble the features the WT spectrum (Figure 7A). Thus the cause of the impaired activity is likely to be a structural perturbation.

(b) G101W. This mutant has been characterized as having its *in vitro* inhibition of cdk4 activity and its *in vivo* binding to cdk4 moderately impaired (Yang et al., 1995) but still competent to arrest cells upon transfection (Koh et al., 1995). The proton NMR spectrum in Figure 7E is the most highly perturbed among all mutants studied. It can be caused by structural perturbation and/or aggregation. The NMR spectrum is too much perturbed to be analyzed; however, the change in the *m* value in Table 2 suggests a possible structural perturbation.

(c) D84N and D84H. D84N effectively inhibits cdk4/cyclin D1 activity *in vitro* but causes only partial arrest of cells upon microinjection (Koh et al., 1995). In consistence with this relatively minor change of activity, its conformation and conformational stability are essentially unperturbed. D84H also shows little perturbation in the conformation and conformational stability. It has not been functionally characterized.

A particularly interesting property of the D84H mutant is that the single mutation enhances the aggregation of the protein, as shown in Figure 10. Even though enhanced aggregation could also occur in other mutants, such as P114L and G101W, the latter cases were not unequivocal since the entire NMR spectra were severely altered. The conformation of D84H was not perturbed, and the increased aggregation is evidently the result of the single mutation.

Conclusion. This work represents the first detailed characterization and structural analyses of the important tumor suppressor p16/Δ1−8 and its mutants. The major findings include the strong tendency of the protein to aggregate, the total NMR assignments under very unfavorable conditions, the determination of secondary structures including ankyrin repeat units, and the correlation between structure and function for four mutants.

ACKNOWLEDGMENT

We are thankful to Dr. Frits Abildgaard for recording HNCACB, CBCA(CO)NH, and 4D $^{13}C/^{13}C$ edited NOESY spectra at 750 MHz, to Robert Hondal and Dr. John Lutton for recording MALDI-TOF mass-spectra, and to Jinling Xie for HeLa cells.

SUPPORTING INFORMATION AVAILABLE

Two tables containing the acquisition parameters for NMR experiments (Table 1) and the ^{1}H, ^{13}C, and ^{15}N resonance assignments (Table 2) of p16/Δ1−8 (9 pages). Ordering information is given on any current masthead page.

REFERENCES

Aves, S. J., Durkacz, B. W., Carr, A., & Nurse, P. (1985) *EMBO J. 4*, 457−463.

Bates, S., Bonetta, L., MacAllan, D., Parry, D., Holder, A., Dickson, C., & Peters, G. (1994) *CDK6* (PLSTIRE) and *CDK4* (PSK-J3) Are a Distinct Subset of the Cyclin-Dependent Kinases That Associate with Cyclin D1. *Oncogene 9*, 71−79.

Bax, A., & Davis, D. G. (1985) *J. Magn. Reson. 65*, 355−360.

Bax, A., & Icura, M. (1991) *J. Biomol. NMR 1*, 99−104.

Bax, A., & Pochapsky, S. (1992) *J. Magn. Reson. 99*, 638−643.

Bax, A., Ikura, M., Kay, L. E., Torchia, D. A., & Tschudin, R. (1990a) *J. Magn. Reson. 86*, 304−318.

Bax, A., Clore, G. M., & Gronenborn, A. M. (1990b) *J. Magn. Reson. 88*, 425−431.

Bodenhausen, G., & Ruben, D. J. (1980) *Chem. Phys. Lett. 69*, 185−189.

Cairns, P., Mao, L., Merlo, A., Lee, D. J., Schwab, D., Eby, Y., Tokino, K., van der Riet, P., Blaugrund, J. E., & Sidransky, D. (1994) Rates of p16 (MTS1) Mutations in Primary Tumors with 9p Loss, *Science 265*, 415−416.

Caldas, C., Hahn, S. A., de Costa, L. T., Redston, M. S., Schutte, M., Seymour, A. B., Weinstein, C. L., Hruban, R. H., Yeo, C. J., & Kern, S. E. (1994) Frequent Somatic Mutations and Homozygous Deletions of the p16 (*MTS1*) Gene in Pancreatic Adenocarcinoma, *Nature Genet. 8*, 27−32.

Cantor, C. R., & Schimmel, P. R. *Biophysical Chemistry, Part II*, W. H. Freeman, & Co., San Francisco.

Chan, F. K. M., Zhang, J., Cheng, L., Shapiro, D. N., & Winoto, A. (1995) Identification of Human and Mouse p19, a Novel CDK4 and CDK6 Inhibitor with Homology to $p16^{INK4A}$, *Mol. Cell Biol. 15*, 2682−2688.

Cordon-Cardo, C. (1995) Mutation of Cell Cycle Regulators. Biological and Clinical Implications for Human Neoplasia, *Am. J. Pathol. 147*, 545−560.

Doherty, A. J., Ashford, S. R., Brannigan, J. A., & Wigley, D. B. (1995) A Superior Host Strain for the Over-Expression of Cloned Genes Using T7 Promoter Based Vectors, *Nucleic Acids Res. 23*, 2074−2075.

Dyson, N. (1994) pRb, p107 and the Regulation of the E2F Transcription Factor, *J. Cell Sci. Suppl. 18*, 81−87.

Gillard, S., Spehner, D., Drillien, R., & Kirn, A. (1986) *Proc. Natl. Acad. Sci. U.S.A. 83*, 5573−5577.

Greenwald, I., & Rubin, G. M. (1992) Making a Difference: The Role of Cell-Cell Interactions in Establishing Separate Identities for Equivalent Cells, *Cell 68*, 271−281.

Grzesiek, S., & Bax, A. (1992a) *J. Magn. Reson. 96*, 432−440.
Grzesiek, S., & Bax, A. (1992b) *J. Am. Chem. Soc. 114*, 6291−6293.
Guan, K.-L., Jenkins, C. W., Li, Y., Nichols, M. A., Wu, X., O'Keefe, C. L., Matera, A. G., & Xiong, Y. (1994) Growth Suppresion by p18, a p16$^{INK4/MTS1}$- and p14$^{INK4B/MTS2}$-Related CDK6 Inhibitor, Correlates with Wild-Type pRb Function, *Genes and Dev. 8*, 2939−2952.
Hannon, J., & Beach, D. (1994) p15^{INK4B} Is a Potential Effector of TGF-b-Induced Cell Cycle Arrest, *Nature 371*, 257−261.
Hartwell, L. H., & Kastan, M. B. (1994) Cell Cycle Control and Cancer, *Science 266*, 1821−1828.
Helps, N. R., Barker, H. M., Elledge, S. J., & Cohen, P. T. (1995) Protein Phosphatase 1 Interacts with p53BP2, a Protein Which Binds to the Tumour Suppressor p53, *FEBS Lett. 377*, 295−300.
Hirai, H., Roussel, M. F., Kato, J.-Y., Ashmun, R. A., & Sherr, C. J. (1995) Novel INK4 Proteins, p19 and p18, Are Specific Inhibitors of the Cyclin D-Dependent Kinases CDK4 and CDK6, *Mol. Cell. Biol. 15*, 2672−2681.
Hopkin, K. (1994) p16/MTS-1: All-Star Tumor Suppressor or Team Player, *J. NIH Res. 6*, 32−36.
Jin, X., Nguyen, D., Zhang, W.-W., Kyritsis, A. P., & Roth, J. A. (1995) Cell Cycle Arrest and Inhibition of Tumor Cell Proliferation by the p16^{INK4A} Gene Mediated by an Adenovirus Vector, *Cancer Res. 55*, 3250−3253.
Kamb, A., Gruis, N. A., Weaver-Feldhaus, J., Liu, Q., Harshman, K., Tavtigian, S. V., Stockert, E., Day III, R. S., Johnston, B. E., & Skolnik, M. H. (1994) A Cell Cycle Regulator Potentially Involved in Genesis of Many Tumor Types, *Science 264*, 436−440.
Kao, L.-R., Peterson, J., Ji, R., Bender, L., & Bender, A. (1996) Interactions between the Ankyrin Repeat-Containing Protein Akr1p and the Pheromone Response Pathway in *Saccharomyces cerevisiae*, *Mol. Cell. Biol. 16*, 168−178.
Kato, J.-Y., Matsuoka, M., Strom, D. K., & Sherr, C. J. (1994) Regulation of Cyclin D-Dependent Kinase 4 (Cdk4) by Cdk4-Activating Kinase, *Mol. Cell. Biol. 14*, 2713−2721.
Kay, L. E., Keifer, P., & Saarinen, T. (1992) *J. Am. Chem. Soc. 114*, 10663−10665.
Kay, L. E., Xu, G.-Y., Singer, A. U., Muhandiram, D. R., & Forman-Kay, J. D. (1993) *J. Magn. Reson. B 101*, 333−337.
Koh, J., Enders, G. H., Dynlacht, B. D., & Harlow, E. (1995) Tumour-Derived p16 Alleles Encoding Proteins Defective in Cell-Cycle Inhibition, *Nature 375*, 506−510.
Kouzarides, T. (1995) Transcriptional Control by the Retinoblastoma Protein, *Semin. Cancer Biol. 6*, 91−98.
Kunkel, T. A. (1985) Rapid and Efficient Site-Specific Mutagenesis without Phenotypic Selection, *Proc. Natl. Acad. Sci. U.S.A. 82*, 488−492.
Lee, K. M., Androphy, E. J., & Baleja, J. D. (1995) A Novel Method for Selective Isotope Labeling of Bacterially Expressed Proteins, *J. Biomol. NMR 5*, 93−96.
Lux, S. E., John, K. M., & Bennett, V. (1990) Analysis of cDNA for Human Erythrocyte Ankyrin Indicates a Repeated Structure with Homology to Tissue-Differentiation and Cell-Cycle Control Proteins, *Nature 344*, 36−42.
Matsuno, K., Diedrich, R. J., Go, M. J., Blaumueller, C. M., & Artavanis-Tsakonas, S. (1995) Deltex Acts as a Positive Regulator of Notch Signaling through Interactions with the Notch Ankyrin Repeats, *Development 121*, 2633−2644.
Matsushime, H., Ewen, M., Strom, D. K., Kato, J.-Y., Hanks, S. K., Roussel, M. F., & Sherr, C. J. (1992) Identification and Properties of an Atypical Catalytic Subunit (p34^{PSK-J3}/cdk4) for Mammalian D Type G1 Cyclins, *Cell 71*, 323−334.
Meyerson, M., & Harlow, E. (1994) Identification of G1 Kinase Activity for Cdk6, a Novel Cyclin D Partner, *Mol. Cell. Biol. 14*, 2077−2086.
Muchmore, D. C., McIntosh, L. P., Russell, C. B., Anderson, D. E., & Dahlquist, F. W. (1989) Expression and Nitrogen-15 Labeling of Proteins for Proton and Nitrogen-15 Nuclear Magnetic Resonance, *Methods Enzymol. 177*, 44−73.
Muhandiran, D. R., & Kay, L. E. (1994) *J. Magn. Reson. B 103*, 203−216.
Muhandiran, D. R., Xu, G.-Y., & Kay, L. E. (1993) *J. Biomol. NMR 3*, 463−70.
Müller, R. (1995) Transcriptional Regulation during the Mammalian Cell Cycle, *Trends Genet. 11*, 173−178.
Ohta, M., Nagai, H., Shimizu, M., Rasio, D., Berd, D., Mastrangelo, M., Singh, A. D., Shields, J. A., Shields, C. L., Croce, C. M., & Huebner, K. (1994) Rarity of Somatic and Germline Mutations of the Cyclin-Dependent Kinase 4 Inhibitor Gene, CDK4I, in Melanoma, *Cancer Res. 54*, 5269−5272.
Okamoto, A., Demetrick, D. J., Spillare, E. A., Hagiwara, K., Hussain, S. P., Bennett, W. P., Forrester, K., Gerwin, B., Serrano, M., Beach, D., & Harris, C. C. (1994) Mutations and Altered Expression of p16^{INK4} in Human Cancer, *Proc. Natl. Acad. Sci. U.S.A. 91*, 11045−11049.
Pace, C. N. (1986) Determination and Analysis of Urea and Guanidine Hydrochloride Denaturation Curves, *Methods Enzymol. 131*, 266−280.
Piotto, M., Saudek, V., & Sklenár, V. (1992) *J. Biomol. NMR 2*, 661−666.
Quelle, D. E., Ashmun, R. A., Hannon, G. J., Rehberger, P. A., Trono, D., Richter, K. H., Walker, C., Beach, D., Sherr, C. J., & Serrano, M. (1995) Cloning and Characterization of Murine p16^{INK4A} and p15^{INK4B} Genes, *Oncogene 11*, 635−645.
Ranade, K., Hussussian, C. J., Sikorski, R. S., Varmus, H. E., Goldstein, A. M., Tucker, M. A., Serrano, M., Hannon, G. J., Beach, D., & Dracopoli, N. C. (1995) Mutations Associated with Familial Melanoma Impair p16^{INK4} Function, *Nature Genet. 10*, 114−116.
Sambrook, J., Fritsch, E. F., & Maniatis, T. (1989) *Molecular Cloning. A Laboratory Manual*, Cold Spring Harbor Laboratory Press, Cold Spring Harbor, NY.
Schägger, H., & von Jagow, G. (1987) Tricine-Sodium Dodecyl Sulfate−Polyacrylamide Gel Electrophoresis for the Separation of Proteins in the Range from 1 to 100 kDa, *Anal. Biochem. 166*, 368−379.
Serrano, M., Gómez-Lahoz, E., DePinho, R. A., Beach, D., & Bar-Sagi, D. (1995) Inhibition of Ras-Induced Proliferation and Cellular Transformation by p16^{INK4A}, *Science 267*, 249−252.
Serrano, M., Hannon, G. J., & Beach, D. (1993) A New Regulatory Motif in Cell-Cycle Control Causing Specific Inhibition of Cyclin D/Cdk4, *Nature 366*, 704−707.
Serrano, M., Lee, H.-W., Chin, L., Cordon-Cardo, C., Beach, D., & DePinho, R. A. (1996) *Cell 85*, 27−37.
Shaka, A. J., Lee, C. J., & Pines, A. (1988) *J. Magn. Reson. 77*, 274−293.
Shpaer, E. G. (1986) *J. Mol. Biol. 188*, 555−564.
Sklenar, V., Piotto, M., Leppik, R., & Saudek, V. (1993) *J. Magn. Reson.*, 241−245.
Spera, S., & Bax, A. (1991) *J. Am. Chem. Soc. 113*, 5490−5492.
Srinvasan, P. R., & Lichter, R. L. (1977) *J. Magn. Reson. 28*, 227−234.
Suzuki-Takahashi, I., Kitagawa, M., Saijo, M., Higashi, H., Ogino, H., Matsumoto, H., Taya, Y., Nishimura, S., & Okuyama, A. (1995) The Interactions of E2F with pRb and with p107 Are Regulated via the Phosphorylation of pRb and p107 by a Cyclin-Dependent Kinase, *Oncogene 10*, 1691−1698.
Tsai, M.-D., & Yan, H. (1991) *Biochemistry 30*, 6806−6818.
Vuister, G. W., Clore, G. M., Gronenborn, A. M., Powers, R., Garrett, D. S., Tshudin, R., & Bax, A. (1993) *J. Magn. Reson. B 101*, 210−213.
Weinberg, R. A. (1995) The Retinoblastoma Protein and Cell Cycle Control, *Cell 81*, 323−330.
Whyte, P. (1995) The Retinoblastoma Protein and Its Relatives, *Semin. Cancer Biol. 6*, 83−90.
Wishart, D. S., Sykes, B. D., & Richards, F. M. (1991) *FEBS Lett. 193*, 72−80.
Wishart, D. S., Bigam, C. G., Holm, A., Hodges, R. S., & Sykes, B. D. (1995) *J. Biomol. NMR 5*, 67−81.
Wittekind, M., & Mueller, L. (1993) *J. Magn. Reson. B 101*, 201−205.
Wüthrich, K. (1986) Familial Melanoma and p16−a Hung Jury, *NMR of Proteins and Nucleic Acids*, John Wiley & Sons, Inc., New York.
Yang, R., Gombart, A. F., Serrano, M., & Koeffler, H. P. (1995) Mutational Effects on the p16^{INK4A} Tumor Suppressor Protein, *Cancer Res. 55*, 2503−2506.

BI960211+